Si(557)-Ag: A metallic quasi-one-dimensional system

J. A. Lipton-Duffin,* A. G. Mark, J. M. MacLeod,* and A. B. McLean
Department of Physics, Engineering Physics and Astronomy, Queen's University, Kingston, Ontario, Canada K7L 3N6
(Received 21 January 2008; published 21 March 2008)

A quasi-one-dimensional (1D) system was fabricated by adsorbing one-fifth of a monolayer of Ag onto a Si(557) surface. Structural investigations performed with electron diffraction and scanning tunneling microscopy provided evidence of a midterrace row of Si adatoms with $2\times$ periodicity along $[1\bar{1}0]$, parallel to the step edges. A similar feature is also found in the Si(557)-Au system. Period doubling along $[1\bar{1}0]$ is also found in the Si(557)-Au system. However, the lattice gas of *extra* Si adatoms, that is a distinctive feature of Si(557)-Au [J. N. Crain *et al.*, Phys. Rev. Lett. **90**, 176805 (2003)], is absent in Si(557)-Ag. Inverse photoemission studies of the Si(557)-Ag energy bands revealed a Fermi level crossing parallel to the step edges along $\overline{\Gamma K}$ at 0.5 ± 0.1 Å^{-1}. In the orthogonal direction ($\overline{\Gamma M'}$), the dispersion of this band is flat, indicating that the adlayer system has a quasi-1D symmetry. Another state with anisotropic dispersion is free-electron-like along $\overline{\Gamma K}$ but, once again, flat along $\overline{\Gamma M'}$. This is likely to be an image state that is in resonance with the bulk bands of Si and also perturbed by the quasi-1D surface reconstruction.

DOI: 10.1103/PhysRevB.77.125419 PACS number(s): 73.20.At, 73.20.−r, 73.21.Hb

I. INTRODUCTION

Much of what we know about the nonlinear and anisotropic electrical properties, elastic properties, and the rich dynamical behavior of low-dimensional charge density wave systems is derived from the study of crystals composed of weakly coupled layers [quasi-two-dimensional (2D)] or weakly coupled rods [quasi-one-dimensional (1D)].[1,2] However, low-dimensional systems can also be grown on surfaces and in some cases, these systems possess structural phase transitions into ground states with broken translational symmetry.[3–5] Quasi-1D adlayer systems can be grown on both low index Si surfaces, e.g. (111), and higher index Si surfaces with steps, e.g. (335), (557), (553), or (775).[6] These stepped surfaces often contain structural motifs that are found in the honeycomb-chain surface reconstructions.[7,8] For example, Si(557)-Au reconstructs so that the step is an integral part of the unit cell and, unlike the steps on low index silicon surfaces, extremely straight (Fig. 1). The Si atoms at the step edge rebond to produce a honeycomb chain (Fig. 1) in which the thermal excitation of kinks is energetically unfavorable. Additionally, rows of Au atoms grow parallel to and in between the step edges. The Si(557)-Au system is metallic at room temperature.[6,9–15] It undergoes a phase transition saturating at 120 K,[16] into a nonmetallic ground state. Despite having only one Au atom in the 1×1 unit cell, Si(557)-Au has two highly dispersive and parallel bands just below the Fermi level.[11,16] It has recently been demonstrated,[15] in agreement with an earlier theoretical prediction,[14] that these two bands are produced by the spin-orbit interaction. A similar effect is found in the *sp*-derived surface states of Au(111).[17] Although this effect is forbidden in the bulk, the absence of an inversion center at the surface allows the spin degeneracy to be lifted.

In this paper we describe our studies of a previously unreported quasi-1D system, Si(557)-Ag, produced by adsorbing 0.2 ML of Ag on Si(557). We proffer that this system is a valuable addition to the small number of metallic quasi-1D adlayer systems that have been discovered to date. From the outset, we expected that the system would have some points of similarity with Si(557)-Au; after all both Ag ($[Kr]4d^{10}5s^1$) and Au ($[Xe]4f^{14}5d^{10}6s^1$) are noble metals with a single *s* shell. However, because Ag is lighter than Au, spin-orbit splitting of the surface bands should be *smaller* in Si(557)-Ag if the atomic geometries of the two surface reconstructions are similar.

II. EXPERIMENT

The samples for these experiments were prepared by dicing rectangles, 6×17 mm^2, from a Si(557) wafer (Virginia Semiconductor). After transfer into vacuum, they were degassed by resistive heating, using a slow overnight ramp from room temperature to 850 °C. The samples were subsequently flashed several times to 1250 °C then quickly cooled to 850 °C, and held at this temperature for 10 min to promote the formation of long-range order. They were then cooled to room temperature at a rate of $\simeq1$ °C/s. The samples were subsequently transferred into a preparation

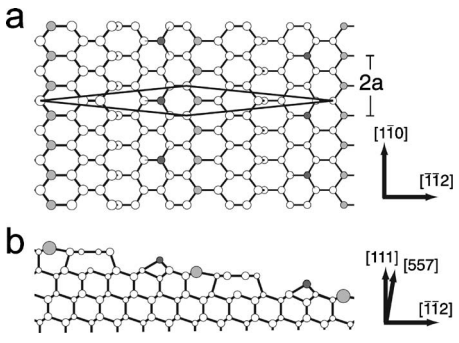

FIG. 1. (a) Top and (b) side views of a model for the Si(557)-Au surface reconstruction (Ref. 6). The solid lines in (a) define the 1×1 unit cell that contains a single Au atom (full light gray circles). The dark light gray circles are Si adatoms and the white circles are Si atoms.

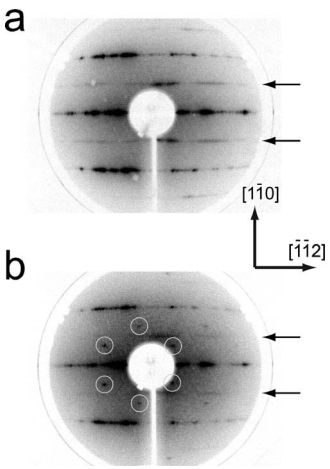

FIG. 2. Electron diffraction images of Si(557)-Ag, taken with a primary beam energy of 80 eV. In (a) the Ag coverage θ=0.2 ML and in (b) θ=0.3 ML. The arrows point out streaks indicated $\times 2$ ordering. The white circles indicate the position of spots produced by diffraction from a $(\sqrt{3}\times\sqrt{3})R30°$ superlattice.

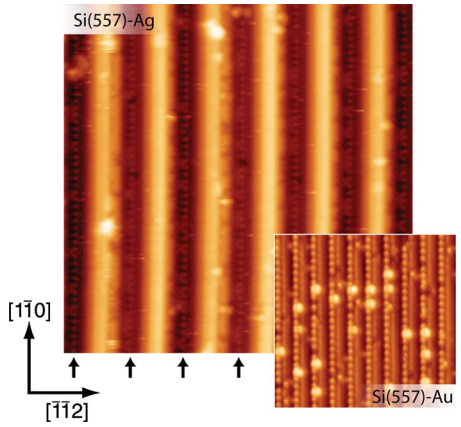

FIG. 3. (Color online) An STM image of Si(557)-Ag, sampling empty states, with an area of 35×35 nm^2 collected using a bias of +1.8 V measured with respect to the tip. The inset shows an image from a Si(557)-Au surface at the same scale and in the same bias range (+1.9 V). The arrows indicate rows of adatoms. The step spacing is three times longer for Si(557)-Ag than for Si(557)-Au.

chamber where they were resistively heated to ≈580 °C while Ag was deposited from an effusion cell. The deposition rate was typically 1 ML/min and the Ag coverage was 0.2 ML.

The inverse photoemission experiments were performed with a homebuilt system comprising a Johnson low energy electron source[18] and two isochromat photon detectors. The detectors are run concurrently to maximize photon detection.[19–22] They have a detection energy of $\hbar\omega_d = 10.61 \pm 0.03$ eV and a full width at half maximum bandpass of $\Delta\hbar\omega_d = 0.37 \pm 0.05$ eV. The energy resolution of the inverse photoemission system does not allow the known[15] spin-orbit splitting (≈0.2 eV) of the Si(557)-Au surface energy bands to be resolved. Consequently, we would not expect to resolve spin-orbit splitting of the surface bands in Si(557)-Ag, if present.

The scanning tunneling microscopy was performed on a homebuilt, beetle-type microscope[23,24] using a mechanically formed Pt-Ir tip with the sample at room temperature.

III. RESULTS AND DISCUSSION

Low energy electron diffraction (LEED) patterns collected from Si(557)-Ag with Ag coverages equal to 0.2 and 0.3 ML are shown in Fig. 2. The intense streaks indicate $1\times$ ordering in the direction parallel to the step edges while the the fainter streaks indicate $2\times$ ordering in the same direction. On Si(557)-Au, the $2\times$ order is caused by Si adatoms that are represented by dark gray circles in Fig. 1.[6,25] The lack of adatom registry between the terraces is responsible for elongating the diffraction spots into streaks.

When the Ag coverage is increased to 0.3 ML, additional spots appear indicating the presence of the $(\sqrt{3}\times\sqrt{3})R30°$ phase [Fig. 2(b)]. Because the $(\sqrt{3}\times\sqrt{3})R30°$ domains form on the (111) terraces, their diffraction pattern is rotated by 9.5°, the angle included by the (111) and (557) surface normals. The results presented in the remainder of this paper are taken from samples with 0.2 ML Ag where the $(\sqrt{3}\times\sqrt{3})R30°$ phase, as judged by LEED, is absent. A constant-current topographical scanning tunneling microscopy (STM) image of the Si(557)-Ag surface is presented in Fig. 3. Black arrows indicate the position of Si adatom rows that are oriented parallel to the step edges. Within the rows, the atoms are spaced by 7.7 Å, twice the Si(111) surface lattice constant (a=3.84 Å). These adatoms give rise to the $2\times$ streaking seen in the LEED patterns.

The step spacing on Si(557)-Au (Ref. 26) can be conveniently expressed in terms of the distance, measured along [$\bar{1}\bar{1}$2], between adjacent nearest neighbor rows on bulk terminated Si(111); $d=a\frac{\sqrt{3}}{2}$. Ideal Si(557) termination has (111) terraces with single-height steps separated by $5\frac{2}{3}d$. The spacing between the adatom rows in Fig. 3 is 5.73 nm equal to $3\times 5\frac{2}{3}d\cos(9.45°)$; the cosine factor projects the oblique "viewing" angle of the STM. This is the step spacing found on Si(557) where the terraces are separated by triple-height steps. Examination of large scale images of Si(557)-Ag confirms that although these are the dominant step type, totaling ~70% of the surface area, there are a large number of steps with a smaller spacing. This behavior is not observed on clean Si(557) or on Si(557)-Au; the step spacing on both of these systems is uniform.[26] In the case of Si(557), the wide terraces allow the formation of a single unit cell of 7×7. Adding Au breaks up the terraces, with single-height steps, and produces terraces with a width of $5\frac{2}{3}d$.

However, it should be noted that the procedure used to prepare Si(557)-Ag differs from the procedure used to prepare Si(557)-Au. To avoid desorbing Ag from the surface, the system was not annealed after Ag deposition because the Ag desorption temperature is significantly lower than the Au desorption temperature.[27,28]

It is also noted that the refaceting effect of Au on vicinal Si(111) is well known. Aside from the aforementioned step breaking action of Au on Si(557), Au has been observed to

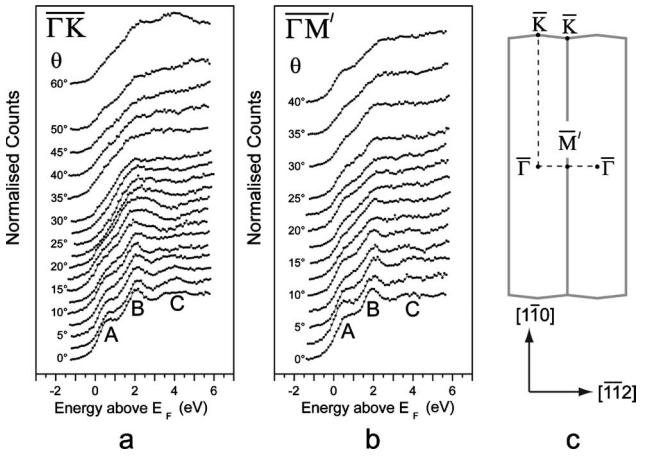

FIG. 4. Inverse photoemission energy distribution curves from Si(557)-Ag sampling (a) $\overline{\Gamma K}$ and (b) the orthogonal $\overline{\Gamma M'}$ direction. (c) Two 1×1 surface Brillouin zones for Si(557), in the extended zone representation, and the principal symmetry points: $\bar{\Gamma}$, $\bar{K}$, and $\bar{M}'$. The red curve in (a) shows the numerical second derivative with respect to energy of the spectrum labeled 0°; this is used to generate the experimental band structures, $(E,k_{\|})$, in the figures below.

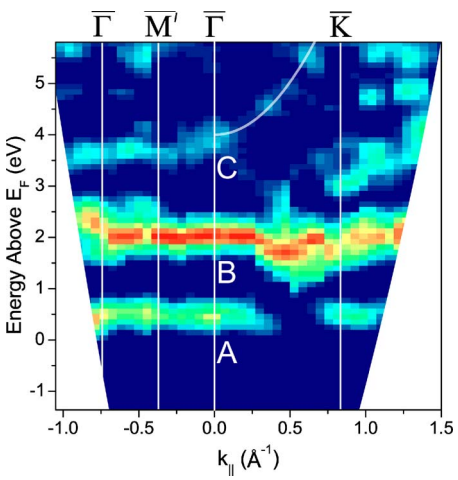

FIG. 5. (Color online) A panel plot of the experimental energy bands for Si(557)-Ag along both $\overline{\Gamma K}$ and $\overline{\Gamma M'}$ calculated from the energy distribution curves of Fig. 4. The faint white line is a parabolic fit to state C.

induced facetting on Si(55 12) even in cases of low coverage and anneal temperatures.[29–31] On the other hand, submonolayer Ag coverage on Si(55 12) under similar conditions does not lead to surface refaceting; the step periodicity remains the same as the clean surface.[32] The case examined here, Si(557)-Ag, lies somewhere in between. The step spacing is largely unperturbed from the clean surface, but some of the triple-height steps do fragment into single- and double-height steps. This has important implications for data interpretation, and we will return to this point when we discuss the results of the inverse photoemission studies that will be presented next.

In Fig. 4(a) stack of inverse photoemission energy distribution curves that sample the $\overline{\Gamma K}$ symmetry direction is presented. The corresponding direction in real space is [1$\bar{1}$0]. The symmetry labels that have been adopted, using a convention introduced earlier,[12] are those of the Si(557)(1×1) surface unit cell [Fig. 4(c)]. Each spectrum was taken with a different incident angle for the electron beam over the angular range $0\leqslant\theta\leqslant60°$. A stack that samples the orthogonal $\overline{\Gamma M'}$ direction is presented in Fig. 4(b). In this case, the angular range was $0\leqslant\theta\leqslant40°$. The energy distribution curves have been offset for clarity.

In both Figs. 4(a) and 4(b), there are three distinct features visible in the $\theta=0°$ spectra labeled A, B, and C. Feature C comprises two components to be discussed later. In Fig. 4(a), as the angle of incidence is increased, the projection of the electron wave vector $(k_{\|})$ along $\overline{\Gamma K}$ is also increased. The state nearest the Fermi level (A) is observed to disperse downward toward the Fermi level and cross the Fermi level at $\theta\approx20°$. Some intensity at the Fermi level is recovered in the spectrum labeled $\theta=50°$ where there is a well-defined shoulder located approximately at $E_F+0.5$ eV. However, there is no *a priori* reason to believe that these two features are produced by the contiguous dispersion of single band below the Fermi level (we will return to this below). The state labeled B has a very shallow dispersion, dipping toward the Fermi level in the spectrum labeled $\theta=15°$ but recovering by $\theta=25°$.

In Fig. 4(b) the orthogonal $\overline{\Gamma M'}$ direction is probed; in real space, the corresponding direction is [$\bar{1}\bar{1}$2]. In contrast to the behavior in the $\overline{\Gamma K}$ direction, the features A, B, and C all have flat dispersion confirming the quasi-1D system character of this system.

The stacked energy distribution curves (EDC) [Figs. 4(a) and 4(b)] do not allow the experimental bands to be viewed directly in reciprocal space. This is straightforwardly achieved by differentiating each EDC twice with respect to energy to pick out regions of high curvature and then mapping the energy distribution curves onto an $(E,k_{\|})$ grid [Fig. 5]. This approach is commonly used to render energy distribution curves acquired with angle-resolved photoemission as experimental band structures.[6,33] Wherever possible we compare the experimental bands of the Si(557)-Ag adlayer system with the experimental bands from the underlying Si(557) surface. This allows us to differentiate substrate features from features associated with the overlayer.

In Fig. 5, the three features (A, B, and C) discussed above are identified as the three bands at $\bar{\Gamma}$. Like Si(557)-Au, there is no evidence of the surface bands backfolding, despite the fact that period doubling is observed in LEED and STM.[6,25] Examination of the intensity just above the Fermi level in Fig. 5 (feature A) reveals the Fermi level crossing at $\approx\frac{1}{2}\overline{\Gamma K}$.

Figure 6 shows the experimental bands for Si(557)-Ag (two right-hand panels; $k_{\|}>0$) plotted, for comparison, "back to back" with the experimental bands for Si(557) (two left-hand panels: $k_{\|}<0$). Based upon a comparison of our experimental bands with the *ab initio* bands for Si(557)-Au,[14] it is possible that the feature near the zone boundary, located just above the Fermi level, arises from an unoccupied Si adatom [Fig. 1(a)] band whereas feature A located near the zone center is produced by a dispersing

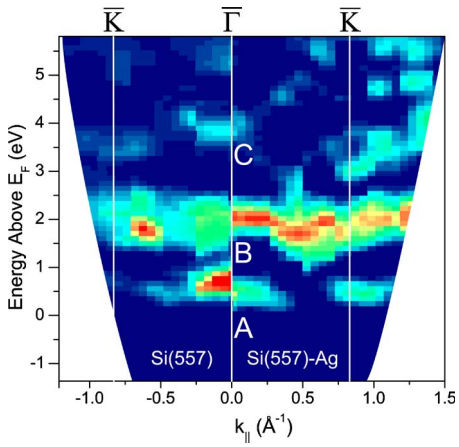

FIG. 6. (Color online) The experimental bands for Si(557)-Ag mapped along $\bar{\Gamma}\bar{K}$ are presented in the two right-hand panels for which $k_{\parallel}>0$. For comparison, the experimental bands for Si(557) also along $\bar{\Gamma}\bar{K}$ are presented, mirror reflected ($k_{\parallel}\rightarrow -k_{\parallel}$), in the two left-hand panels for which $k_{\parallel}<0$.

Si-Ag band.[14] The presence of an additional adatom band at the zone boundary, absent on Si(557)-Au,[25] may reflect a difference in the atomic geometry of the terrace.

The feature labeled B is produced by the adsorption of Ag and closely resembles features produced by adsorbing Ag on Si(111).[34,35] The state dispersion is shallow along $\bar{\Gamma}\bar{K}$, the state moving to slightly larger binding energy around $\frac{1}{2}\bar{\Gamma}\bar{K}$, and flat along $\bar{\Gamma}\bar{M}'$. The experimental bands from Si(557)-Ag, and also from our earlier studies of Si(557)-Au,[25] can be directly compared in Fig. 7. Clearly the electronic structure of these two systems is similar. The Fermi level crossing in both systems is located at $k_{\parallel}\approx 0.5\pm 0.1$ Å^{-1} and the dispersion of feature B is almost identical.

The feature labeled C, located at $\approx E_F+4$ eV at $\bar{\Gamma}$, is found to disperse parabolically, along $\bar{\Gamma}\bar{K}$, toward lower binding energy. Fitting a parabola to the band dispersion produces an effective mass close to the free-electron mass $m^*=(0.96\pm 0.04)m_e$ and places the band minimum 0.6 ± 0.4 eV below the vacuum level. There is an analogous state in the Si(557)-Au system.[25] As with features A and B, the dispersion of C is flat along $\bar{\Gamma}\bar{M}'$ suggesting that state C "feels" the surface corrugation associated with the quasi-1D surface structure. The width of this state, at $\bar{\Gamma}$, reflects the fact that there are contributions from two separate states, one being the image state resonance and the other being a radiative transition into the Λ_3 bulk band of Si. The two contributions are resolved in Fig. 4(a) and both the image state and the bulk transition have been discussed in detail elsewhere in the context of Si(557)-Au.[25]

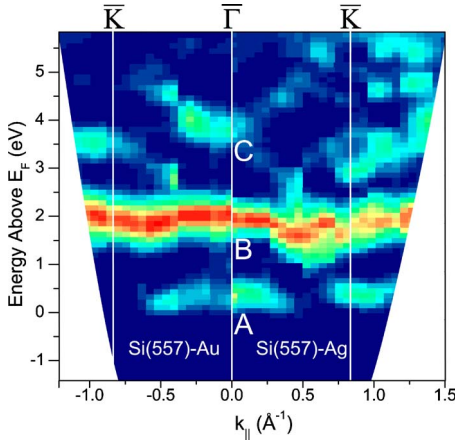

FIG. 7. (Color online) The experimental bands for Si(557)-Ag along $\bar{\Gamma}\bar{K}$ are presented in the two right-hand panels ($k_{\parallel}>0$) and, for comparison, the corresponding bands from Si(557)-Au, mirror reflected ($k_{\parallel}\rightarrow -k_{\parallel}$), in the two left-hand panels ($k_{\parallel}<0$).

The partial breakup of the steps into single-height and double-height steps, which we have observed via STM on Si(557)-Ag, complicates the interpretation of the inverse photoemission spectra. Moreover, this is a surface reconstruction. The surface geometry is unknown and no *ab initio* calculations have yet been performed. Despite all of the above, we can draw some conclusions from the striking similarity that the experimental energy bands of Si(557)-Au and Si(557)-Ag bear. For example, it is likely that the intense band that disperses across the Fermi level is produced by the hybridization of the Ag atoms with the Si atoms on the majority terrace. It is also likely that feature B is a Ag-Si adatom band and feature C is an image state resonance. However, we run into difficulty when we try to assign the experimental band that appears at the zone edge, because there are no corresponding bands in this region of reciprocal space on Si(557)-Au. Consequently there may be a difference in the atomic geometry, a prime candidate being the minority terraces of Si(557)-Ag. Clearly further structural studies are required to identify the atomic geometry of Si(557)-Ag and allow *ab initio* calculations of the surface electronic structure to be performed. Moreover, it is our belief that local studies of this system using scanning tunneling spectroscopy will be extremely helpful.

CONCLUSION

We have reported on a quasi-one-dimensional overlayer system formed from Ag on Si(557). Despite the fact that this system has some points of similarity with Si(557)-Au, there are also some noticeable differences. Examples of the similarities include straight step edges and rows of adatoms with $2\times$ spacing running parallel to the step edges, strongly anisotropic, quasi-1D unoccupied electronic structure, a Fermi level crossing at 0.5 ± 0.1 Å^{-1} in the direction that lies parallel to the Si adatom rows ($\bar{\Gamma}\bar{K}$), and a band 0.6 ± 0.4 eV below the vacuum level at $\bar{\Gamma}$ that is most likely a quasi-1D image state in resonance with the bulk band structure of Si. Differences include the "missing" lattice gas of extra Si adatoms that are a distinctive feature of Si(557)-Au (Ref. 36), and a dominant step spacing of 5.73 nm, three times the Si(557)-Au step spacing.

The Si(557)-Ag system is clearly an intriguing companion to Si(557)-Au because it shares some, but not all, of its attributes. Consequently, it will allow many of the ideas that have been developed over the past decade to explain the

structural and electronic properties of Si(557)-Au to be tested. Do the structural differences arise from substituting Ag for Au, and do they account for the lack of the lattice gas of Si adatoms, the increased step spacing, or the altered electronic properties of the system? Further investigation of the occupied bands, using high resolution photoemission and *ab initio* theory, is required to ascertain the magnitude of the spin-orbit splitting, which cannot be quantified with inverse photoemission, and also determine if Si(557)-Ag possesses a phase transition into a nonmetallic ground state with broken translational symmetry.

ACKNOWLEDGMENTS

This research was supported by the Natural Sciences and Engineering Research Council of Canada.

*Present address: Institut National de Recherche Scientifique-EMT, 1650 Boulevard Lionel-Boulet, Varennes, Québec, Canada J3X 1S2.

[1] J. A. Wilson, F. J. D. Salvo, and S. Mahajan, Phys. Rev. Lett. **32**, 882 (1974).
[2] R. E. Thorne, Phys. Today **49** (5), 42 (1996).
[3] E. Tosatti, *Electronic Surface and Interface States on Metallic Systems*, edited by E. Bertel and M. Donath (World Scientific, Singapore, 1995), p. 67.
[4] P. A. Dowben, Surf. Sci. Rep. **40**, 151 (2000).
[5] T. Aruga, J. Phys.: Condens. Matter **14**, 8393 (2002).
[6] J. N. Crain, J. L. McChesney, F. Zheng, M. C. Gallagher, P. C. Snijders, M. Bissen, C. Gundelach, S. C. Erwin, and F. J. Himpsel, Phys. Rev. B **69**, 125401 (2004).
[7] S. C. Erwin and H. H. Weitering, Phys. Rev. Lett. **81**, 2296 (1998).
[8] D. T. Petrovykh, K. N. Altmann, J. L. Lin, F. J. Himpsel, and F. M. Leibsle, Surf. Sci. **512**, 269 (2002).
[9] K. N. Altmann, J. N. Crain, A. Kirakosian, J.-L. Lin, D. Y. Petrovykh, F. J. Himpsel, and R. Losio, Phys. Rev. B **64**, 035406 (2001).
[10] P. Segovia, D. Purdie, M. Hengsberger, and Y. Baer, Nature (London) **402**, 504 (1999).
[11] R. Losio, K. N. Altmann, A. Kirakosian, J.-L. Lin, D. Y. Petrovykh, and F. J. Himpsel, Phys. Rev. Lett. **86**, 4632 (2001).
[12] D. Sánchez-Portal, J. D. Gale, A. García, and R. M. Martin, Phys. Rev. B **65**, 081401(R) (2002).
[13] D. Sánchez-Portal and R. M. Martin, Surf. Sci. **532-535**, 655 (2003).
[14] Daniel Sánchez-Portal, Sampsa Riikonen, and Richard M. Martin, Phys. Rev. Lett. **93**, 146803 (2004).
[15] I. Barke, F. Zheng, T. K. Rugheimer, and F. J. Himpsel, Phys. Rev. Lett. **97**, 226405 (2006).
[16] J. R. Ahn, H. W. Yeom, H. S. Yoon, and I.-W. Lyo, Phys. Rev. Lett. **91**, 196403 (2003).
[17] S. LaShell, B. A. McDougall, and E. Jensen, Phys. Rev. Lett. **77**, 3419 (1996).
[18] N. G. Stoffel and P. D. Johnson, Nucl. Instrum. Methods Phys. Res. A **234**, 230 (1984).
[19] J. Lipton-Duffin, Master's thesis, Queen's University, 2001.
[20] J. A. Lipton-Duffin, A. G. Mark, and A. B. McLean, Rev. Sci. Instrum. **73**, 3149 (2002).
[21] J. A. Lipton-Duffin, A. G. Mark, G. K. Mullins, G. E. Contant, and A. B. McLean, Rev. Sci. Instrum. **75**, 445 (2004).
[22] J. Lipton-Duffin, Ph.D. thesis, Queen's University, 2006.
[23] A. Lucas, Master's thesis, Physikalisches Institut Universität Stuttgart, 2000.
[24] J. M. MacLeod, A. Moffat, J. A. Miwa, A. G. Mark, G. K. Mullins, R. H. J. Dumont, G. E. Constant, and A. B. McLean, Rev. Sci. Instrum. **74**, 2429 (2003).
[25] J. A. Lipton-Duffin, J. M. MacLeod, and A. B. McLean, Phys. Rev. B **73**, 245418 (2006).
[26] A. Kirakosian, R. Bennewitz, J. N. Crain, T. Fauster, J. L. Lin, D. Y. Petrovykh, and F. J. Himpsel, Appl. Phys. Lett. **79**, 1608 (2001).
[27] Akira Endo and Shozo Ino, Jpn. J. Appl. Phys., Part 1 **32**, 4718 (1993).
[28] Shuji Hasegawa, Hiroshi Daimona, and Shozo Ino, Surf. Sci. **186**, 138 (1987).
[29] A. A. Baski and K. M. Saoud, J. Cluster Sci. **12**, 527 (2001).
[30] J. W. Dickinson, J. C. Moore, and A. A. Baski, Surf. Sci. **561**, 193 (2004).
[31] L. Seehofer, S. Huhs, G. Falkenberg, and R. Johnson, Surf. Sci. **329**, 157 (1995).
[32] K. M. Jones, H. H. Song, and A. A. Baski, J. Cluster Sci. **10**, 573 (1999).
[33] T. Abukawa, M. Sasaki, F. Hisamatsu, T. Goto, T. Kinoshita, A. Kakizaki, and S. Kono, Surf. Sci. **325**, 33 (1995).
[34] J. M. Nicholls, F. Salvan, and B. Reihl, Surf. Sci. **178**, 10 (1986).
[35] J. M. Nicholls, F. Salvan, and B. Reihl, Phys. Rev. B **34**, 2945 (1986).
[36] J. N. Crain *et al.*, Phys. Rev. Lett. **90**, 176805 (2003).